

Temperature-dependent line broadening in core-level photoemission spectra from aluminum

W. Theis and K. Horn

Fritz-Haber-Institut der Max-Planck-Gesellschaft, W-1000 Berlin 33, Germany

(Received 29 March 1993)

The temperature dependence of the Al 2*p* line width and binding energy has been studied in the range from 80 K up to and beyond the Al bulk melting point ($T_m = 933.5$ K). By comparing the experimental data with results from calculations based on a nearest-neighbor force constant model, we find the phononic coupling to be of quadratic rather than linear nature as previously assumed. The temperature dependence of the Al 2*p* binding energy is interpreted on the basis of thermal expansion and phononic coupling.

The quantitative study of the line shape of core-level photoemission spectra has given insight into many aspects of solid-state physics.¹ Whereas there is a general understanding of the way in which binding-energy shifts reflect the chemical environment, the Lorentzian width reflects the lifetime of the core hole, and the Doniach-Šunjić asymmetry indicates the metallicity of the sample, studies of the origin of the Gaussian contribution to the linewidth have been very sparse.²⁻⁴ While an inequivalence of the photoemitting atomic cores clearly leads to a broadening of the spectra, the detailed mechanisms involved have yet to be understood. For photoemission from bulk atoms in a perfect single crystal, this inequivalence is caused by phononic excitation of the lattice, density waves of the valence electrons, and other distortions of translational symmetry. Since the dependence of the magnitude of thermal excitations on temperature is well known as outlined below, temperature-dependent studies promise to elucidate the influence of these excitations on the photoemission spectra and thus give insight into the photoemission process itself. It is therefore essential to collect photoemission data over the widest temperature range possible. Here, we present experiments extending above room temperature and beyond the melting point of the metal studied. Furthermore, this is an experimental study at sufficiently high temperature for the effect of electron density waves to become significant.

The photoemission spectra were obtained on the wiggler-undulator beamline at BESSY (Berliner Elektronenspeicherring für Synchrotronstrahlung GmbH) using the TGM5 and TGM6 monochromators at photon energies ranging from 80 to 110 eV. Photoelectrons were collected with a 50-mm radius hemispherical analyzer. The combined overall resolution of monochromator and analyzer was determined *in situ* utilizing a retractable gas cell for photoemission from the Ar 3*p* core level. It was found that after optimization of the monochromator the instrumental transmission function could be approximated to high accuracy by a Gaussian. The best overall resolution was obtained with the TGM6 monochromator yielding a Gaussian of 70 meV full width at half maximum (FWHM) at a photon energy of 82 eV.

The aluminum samples were spark cut from a single-crystal rod and mechanically and electropolished. They were mounted on molybdenum sample holders encasing a ceramic-insulated tantalum coil used for resistive heating. The experiments were performed at a base pressure of 3×10^{-11} mbar. The crystals were cleaned by cycles of neon ion sputtering at room and elevated temperatures and annealing up to 900 K. Chemical and structural surface quality were verified by valence-band photoemission and low-energy electron diffraction. All spectra were recorded at constant sample temperatures. Measurement and heating alternated with a frequency of 30 Hz to guarantee that the photoemission data were not influenced by electric potentials or stray fields.⁵ The temperature stability attained was on the order of 10 mK.

Al 2*p* spectra of the Al(111) and Al(100) surfaces were measured with photon energies between 82 and 110 eV to cover the full range of surface sensitivity as given by the photoelectron's inelastic free path of about 15 to 3 Å, respectively.⁶ For each photon energy several sets of spectra comprising different sample temperatures under otherwise identical experimental conditions were recorded. A typical set of data is shown in Fig. 1. The photoemission spectra consist of a bulk line, a possible surface line, and of background intensity due to inelastic scattering and other processes. The bulk and surface lines are given by broadened spin-orbit split pairs of Doniach-Šunjić lines. The broadening is attained by a convolution of the lines with an appropriately chosen function. We arrived at an excellent description of the experimental spectra by convoluting with Gaussians, which reflects the theoretical understanding of the underlying processes, as will be expanded upon later. The inelastic scattering of Al 2*p* photoelectrons gives a contribution to the background increasing linearly in intensity with the kinetic-energy loss relative to the elastic line,⁷ while the other processes not directly connected to the emission from the Al 2*p* level were accounted for by a polynomial contribution to the background.

Due to thermal expansion and interaction with phonons one expects the binding energy and Gaussian broadening to be temperature dependent. All other pa-

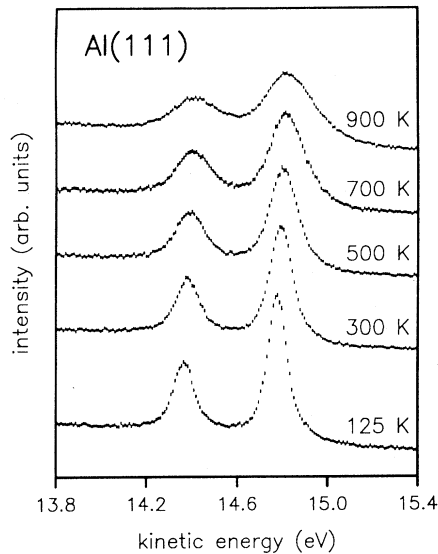


FIG. 1. Al 2*p* photoemission spectra from Al(111) recorded with a photon energy of $\hbar\omega=82$ eV and an instrumental resolution of 70 meV at different temperatures.

rameters are independent of sample temperature and were held fixed at the following values in the fit of all spectra. The Lorentzian width was determined to be 30 meV FWHM with a lower limit of 25 meV and an upper limit of 40 meV. The latter limit was inferred from the knowledge of the instrumental resolution as gained by *in situ* gas phase photoemission of the Ar 3*p* level. The Lorentzian width is smaller than those used by other authors to fit their spectra,^{8,2} but agrees better with even slightly smaller calculated values for *sp* metals.⁹ The spin-orbit splitting used was 411 meV, having been determined to within an accuracy of ± 2 meV. A Doniach-Šunjić asymmetry parameter α between 0.075 and 0.110 was found to describe the measured spectra satisfactorily. With theoretical values $\alpha=0.13$,¹⁰ 0.11,¹¹ and 0.10 (Ref. 12) in the higher range, we have used in our analysis $\alpha=0.1$ which yields excellent agreement between spectra and fits.

Analysis showed that the Al(111) spectra were well described without a separate surface line, while in the case of Al(100) a surface line could be observed unambiguously. We found the surface line in Al(100) to be additionally broadened by 80 ± 20 meV and shifted by -94 ± 5 meV towards lower binding energy with respect to the bulk line. This result is in excellent agreement with recent experimental⁸ and theoretical¹³ results, pointing towards an end to a history of strong controversy on this topic.¹⁴⁻¹⁹

In the spectra of the Al 2*p* line shown in Fig. 1, taken at different temperatures from the Al(111) surface, one can observe a significant broadening, and a small binding-energy shift with increasing temperature. A line-shape analysis as outlined above yields the intrinsic Gaussian (full) width (Fig. 2) by subtracting (quadratically) the instrumental resolution from the observed Gaussian broadening and the binding-energy shift (Fig. 3). In the figures different temperature runs are indicated by

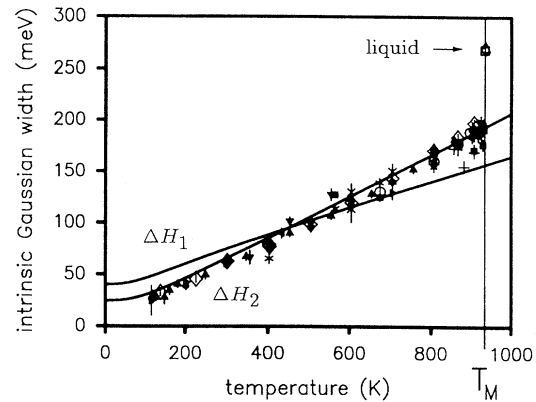


FIG. 2. Intrinsic Gaussian width of the Al 2*p* bulk core level line as a function of temperature, and results of calculations based on linear (ΔH_1) and quadratic phononic coupling (ΔH_2). Rhombi signify data from Al(100), other symbols data from Al(111). Error bars, visible in some of the data points, are equal to one standard deviation.

different symbols with rhombi signifying data from Al(100).

For all sets of spectra an identical dependence of intrinsic width and binding-energy shift on temperature is observed. Since the different sets from Al(111) were taken at a range of photon energies and thereby at strongly differing surface sensitivity, we conclude that the Al(111) surface atoms give a line identical to that of the bulk atoms. The agreement of the Al(100)-derived data with those of Al(111) shows that the Al(100) surface component is correctly described also for higher temperatures where it cannot be extracted directly from the spectra due to the large intrinsic width of the Al 2*p* emission line. A linear increase of intrinsic Gaussian width and binding-energy shift with temperature is observed in the data of Figs. 2 and 3. At the melting point both quanti-

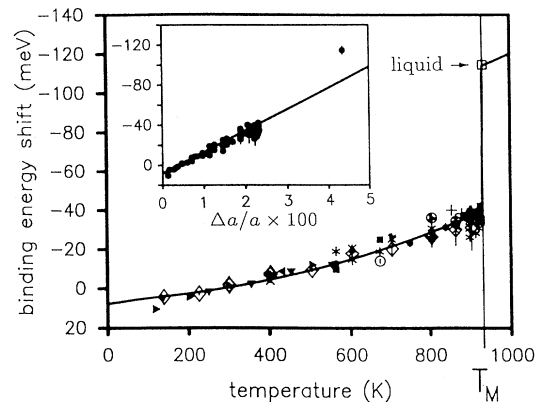


FIG. 3. Binding-energy shifts of the Al 2*p* bulk line relative to the binding energy at 274 K as a function of temperature, compared with results of calculations based on thermal expansion and phononic coupling. Rhombi signify data from Al(100), other symbols data from Al(111). Inset: binding-energy shift vs relative linear expansion. The line corresponds to a linear dependence of binding energy on linear expansion in the region below the melting point.

ties display a discontinuous increase in magnitude.

In core-level photoemission the sudden ionization of the emitting atom causes a major distortion of the homogeneity of the system. During ionization, the density distribution of the valence-band electrons changes in order to screen the extra charge, while the movement of the atoms is much slower, preventing any changes in positions during ionization. At $T=0$, valence-band density waves are excited to screen the ion, resulting in the well-known Doniach-Šunjić asymmetry of photoemission lines in metals.^{20–22} At higher temperatures such density waves are already excited in thermal equilibrium before ionization. Being bosons they are both created and annihilated to the same extent (excluding the $T=0$ contribution) during ionization, causing a symmetric broadening of the asymmetric Doniach-Šunjić photoemission line.⁹ The exact broadening to second order is attained by convoluting the line by the Fourier transformation $g(\omega)$ of the core hole time correlation function (Green's function)⁹

$$g(t) = \left| \frac{\pi t T}{\sinh(\pi t T)} \right|^\alpha. \quad (1)$$

The exponent α is identical to the parameter giving the Doniach-Šunjić asymmetry. In the presence of other broadening mechanisms of similar or greater magnitude, the shape of $g(t)$ remains significant only for small times. In this case $g(t)$ can be approximated by a Gaussian, yielding for the convolution function $g(\omega)$ a Gaussian with full width at half maximum of⁹

$$\Delta = \sqrt{8 \ln(2)} \pi k_B T \sqrt{\alpha/3}. \quad (2)$$

The broadening is proportional to the temperature and fully determined by the Doniach-Šunjić asymmetry parameter α . A temperature-dependent shift of the line due to the mechanism discussed above does not occur.

After ionization the atomic arrangement does not represent the thermal equilibrium any more. It is not even an eigenstate of the lattice with the ion, but a superposition of eigenstates with different energies, resulting in corresponding broadening of the photoemission line. The first moments of the photoemission line can be easily expressed in terms of the change in the lattice Hamiltonian due to the ionization of the photoemitting atom $\Delta H = H_{\text{after}} - H_{\text{before}}$. The first moment, i.e., the shift of the distribution, is $-\langle\langle \Delta H \rangle\rangle$, the second is $\langle\langle (\Delta H)^2 \rangle\rangle$, where $\langle\langle \rangle\rangle$ denotes the thermal average with respect to the Hamiltonian without ion. Neglecting all higher moments, one obtains a Gaussian energy distribution with full width at half maximum of²³

$$\Delta = \sqrt{8 \ln(2)} [\langle\langle (\Delta H)^2 \rangle\rangle - (\langle\langle \Delta H \rangle\rangle)^2] \quad (3)$$

and a shift in binding energy of

$$\Delta E_B = -\langle\langle \Delta H \rangle\rangle. \quad (4)$$

We have performed a model calculation in order to establish the influence of different possible changes in the Hamiltonian due to the creation of an ion in the lattice on the photoemission spectra. In order to maintain a clear physical picture of the principles involved, while

still reflecting the lattice properties of aluminum, we have chosen a nearest-neighbor force constant model of a fcc lattice. The only free parameter, i.e., the force constant, was set to yield the best agreement between the calculated and experimental phonon dispersion.

The first change in the Hamiltonian studied is ΔH_1 resulting from changed equilibrium distances between the ion and its nearest neighbors, the second is ΔH_2 resulting from a change in the respective force constants. ΔH_1 and ΔH_2 are referred to as linear and quadratic coupling, since they are of first and second order in the generalized coordinates, respectively. We have calculated the resulting shift and width of the photoemission lines by analytically transforming these quantities into integrals over expectation values of products of the coordinates describing the normal modes.⁵ While the expectation values are simply given as functions of the energies involved, the integrations over the Brillouin zone were performed by summing over 300 randomly chosen points.

The results of the calculation are indicated as solid lines in Fig. 2 for ΔH_1 and ΔH_2 , respectively. They include the contribution due to the electronic effect [Eq. (2)] based on an asymmetry parameter of $\alpha=0.1$ gained from the line-shape analysis, and the contribution from phonon coupling with the coupling strength chosen for best agreement with the experimental data. The change in nearest-neighbor separation for ΔH_1 is 5.6% (increase and decrease yield identical results), while an increase in force constants of 60% has been assumed for the calculation of ΔH_2 . It is obvious from Fig. 2 that quadratic coupling (ΔH_2) provides an excellent description of the experimental data, while the curve for linear coupling deviates considerably. On the basis of the equivalent core approximation often used for the description of the valence charge for the photoion, an increase in the valence charge from 3 to 4, i.e., by 33% is of similar magnitude to the increase in force constant. Data at high temperature (> 400 K) are particularly relevant for the distinction between the two modes of coupling, as the general shape of the theoretical curves in this region is independent of the details of the underlying model.⁵ For linear coupling, the broadening turns out to be proportional to \sqrt{T} , while for quadratic coupling a linear relationship is predicted, in obvious agreement with the data at high temperatures. It is worth noting that in the only other extensive study of the temperature dependence of photoemission line widths, Riffe, Wertheim, and Citrin⁴ observe a linear phononic coupling for the case of sodium. The difference in coupling mechanism points towards fundamental insights to be gained by studying the broadening of photoemission lines in a larger number of materials.

The observed dependence of the binding energy on the sample temperature is shown in Fig. 3. In discussing it, the effect of thermal expansion of the lattice on the binding energy must be taken into account. The associated reduction in electron density causes changes in conduction-band width, electrostatic potential, and relaxation energy, yielding a linear dependence of binding energy on the relative linear expansion $\Delta a/a$.^{2,24} The plot of binding energy E_B over $\Delta a/a$ in the inset of Fig. 3 does indeed reveal a linear relationship between these

quantities for temperatures below the melting point. An overall linear relationship between E_B and $\Delta a/a$, however, is clearly precluded by the large decrease of E_B upon melting. Consequently, additional mechanisms must be considered to explain the observed temperature dependence of the binding energy. The only viable mechanism is coupling to phonons, which has already been discussed above in connection with the line broadening. While linear coupling has no effect on binding energy, quadratic coupling, which was found to be instrumental in the broadening of the photoemission line, induces a temperature-dependent shift of the binding energy [see Eq. (4)]. If we include this contribution, albeit with a smaller increase in force constant (22%) than used for the description of the broadening above, excellent agreement

is obtained as demonstrated by the solid line in Fig. 3. The assumed shift of -37.5 meV per 1% of linear thermal expansion is in fair agreement with values of -39 and -26 meV gained from formulas by Citrin, Wertheim, and Baer² based on calculations of the polarization energy and by Hedin and Lundquist,²⁵ and by Riffe *et al.*,²⁴ respectively. Since the contributions of thermal expansion and quadratic coupling are quite similar a first-principles calculation of the effect of expansion alone would be of considerable interest.

This work was supported by the Bundesministerium für Forschung und Technologie under Grant No. 055EBFXB.

¹See, for example, *Photoemission in Solids*, edited by M. Cardona and L. Ley, Topics in Applied Physics Vols. 26 and 27 (Springer-Verlag, Berlin, 1978).

²P. H. Citrin, G. K. Wertheim, and Y. Baer, *Phys. Rev. B* **16**, 4256 (1977).

³D. M. Riffe, G. K. Wertheim, and P. H. Citrin, *Phys. Rev. Lett.* **63**, 1976 (1989).

⁴D. M. Riffe, G. K. Wertheim, and P. H. Citrin, *Phys. Rev. Lett.* **67**, 116 (1991).

⁵W. Theis, Ph.D. thesis, Freie Universität Berlin, 1992; (unpublished).

⁶C. J. Tung and R. H. Ritchie, *Phys. Rev. B* **16**, 4302 (1977).

⁷S. Tougaard, *Surf. Interface Anal.* **11**, 453 (1988).

⁸R. Nyholm, J. N. Andersen, J. F. van Acker, and M. Qvarford, *Phys. Rev. B* **44**, 10 987 (1991).

⁹C.-O. Almbladh and P. Minnhagen, *Phys. Status Solidi B* **85**, 135 (1978).

¹⁰C.-O. Almbladh and U. von Barth, *Phys. Rev. B* **13**, 3307 (1976).

¹¹P. Minnhagen, *J. Phys. F* **7**, 2441 (1977).

¹²G. W. Bryant and G. D. Mahan, *Phys. Rev. B* **17**, 1744 (1978).

¹³P. J. Feibelman, *Phys. Rev. B* **39**, 4866 (1989).

¹⁴W. Eberhardt, G. Kalkoffen, and C. Kunz, *Solid State Commun.* **32**, 901 (1979).

¹⁵H. Krakauer, M. Posternak, A. J. Freeman, and D. D. Koelling, *Phys. Rev. B* **23**, 3859 (1981).

¹⁶T.-C. Chiang and D. E. Eastman, *Phys. Rev. B* **23**, 6836 (1981).

¹⁷E. Wimmer, M. Weinert, A. J. Freeman, and H. Krakauer, *Phys. Rev. B* **24**, 2292 (1981).

¹⁸R. Kammerer, J. Barth, F. Gerken, C. Kunz, S. A. Flodström, and L. I. Johansson, *Phys. Rev. B* **26**, 3491 (1982).

¹⁹P. S. Bagus, G. Pacchioni, and F. Parmigiani, *Phys. Rev. B* **43**, 5172 (1991).

²⁰P. Nozières and C. T. De Dominicis, *Phys. Rev.* **178**, 1097 (1969).

²¹S. Doniach and M. Šunjić, *J. Phys. C* **3**, 285 (1970).

²²K. D. Schotte and U. Schotte, *Phys. Rev.* **182**, 479 (1969).

²³C. Kunz, in *Synchrotron Radiation*, edited by C. Kunz (Springer-Verlag, Berlin, 1979).

²⁴D. M. Riffe, G. K. Wertheim, D. N. E. Buchanan, and P. H. Citrin, *Phys. Rev. B* **45**, 6216 (1992).

²⁵L. Hedin and S. Lundquist, in *Solid State Physics*, edited by F. Seitz and D. Turnbull (Academic, New York, 1969), Vol. 23.